Porphyrin-Functionalized Amphiphilic Diblock Copolypeptides for Photodynamic Therapy

ZE-YONG LI, HUI-YUAN WANG, CAO LI, XIAO-LU ZHANG, XIAO-JUN WU, SI-YONG QIN, XIAN-ZHENG ZHANG, REN-XI ZHUO

Key Laboratory of Biomedical Polymers of Ministry of Education, Department of Chemistry, Wuhan University, Wuhan 430072, China

Received 10 August 2010; accepted 19 October 2010
DOI: 10.1002/pola.24451
Published online 18 November 2010 in Wiley Online Library (wileyonlinelibrary.com).

ABSTRACT: A series of amphiphilic diblock copolypeptides (ADCs), 5-(4-aminophenyl)-10,15,20-triphenyl-porphyrin (APP) conjugated poly(L-leucine)-*block*-polylysine (APP-L_nK_m) with different molar ratios of L-leucine unit and lysine unit were designed and synthesized. The optimized composition of the polypeptide was determined to be APP-$L_{109}K_{186}$, which has high fluorescence quantum yield and could self-assemble into micelles in an aqueous medium with mean particle size $<$30 nm. The *in vitro* study indicates that APP-$L_{109}K_{186}$ shows no significant dark cytotoxicity when the concentration is below 200 mg L^{-1} for HepG2 and HeLa cells. In contrast, the polymer exhibits apparent phototoxicity with low IC_{50} values toward HepG2 and HeLa cells, implying that the potential high photodynamic therapy efficacy of the polymer. © 2010 Wiley Periodicals, Inc. J Polym Sci Part A: Polym Chem 49: 286–292, 2011

KEYWORDS: amphiphiles; *N*-carboxyanhydride; drug delivery systems; micelle; polypeptide; phototoxicity; self-organization

INTRODUCTION Photodynamic therapy (PDT) is a promising treatment for many types of tumors, including lung, esophageal, cervical, bladder, and gastric tumors.[1] PDT is based on the tumor-specific accumulation of a photosensitizer (PS), often a porphyrin derivative, followed by irradiation with visible light, which induces the generation of highly reactive oxygen species (ROS) and then leads to irreversible destruction of the treated tissues.[2] For early or localized disease, PDT can be a selective and curative therapy without damaging surrounding healthy tissues. For PDT, PS is a key factor that can absorb light with appropriate wavelength at the site of the photodynamic reaction to produce ROS to mediate cellular toxicity. As the second generation of PS, porphyrin derivatives[3] are extensively studied because they are the effective generators of singlet oxygen with favorable properties such as selectivity for particular diseased tissues and relatively fast elimination from the body, which minimizes side effects.[4] However, most of porphyrin derivatives are hydrophobic. This lipophilic nature may be an important obstacle for the preferential accumulation in cellular hydrophobic loci as these molecules must be able to get into cells by crossing lipid membranes,[5] and thus greatly limits the *in vivo* applications. In addition, because of their chemical structure, most PSs tend to aggregate in aqueous media as a result of the propensity of the hydrophobic skeleton to avoid contact with water molecules,[6] which affect their efficacy *in vivo* due to the decreased bioavailability and capacity to absorb light.[7,8] To overcome this problem, the delivery systems for porphyrin derivatives such as oil-dispersions, liposomes, polymeric particles, hydrophilic polymer, or amphiphilic polymer–PS conjugates have been developed.[4]

Synthesis and polymerizations of α-amino acid *N*-carboxyanhydrides (NCAs) were reported for the first time by Leuchs in 1906.[9] From then on, these cyclic and highly reactive amino acid derivatives have been used for peptide synthesis but mainly for the formation of polypeptides by ring opening polymerizations (ROP).[10] The synthetic polypeptides produced from the NCAs are able to form highly ordered structure such as α-helix and β-sheet. The different self-assembly morphologies could be observed by varying the polypeptide compositions, sequences, and segments length. These polypeptides have good biocompatibility and biodegradability because of the chemical and structural similarity to natural biomolecules such as proteins.

In aqueous medium, amphiphilic block copolymers possess the ability to spontaneously self-assemble into nanosized micelles with a typical core-shell structure with attractive properties as promising colloidal carriers for poorly water-soluble and amphiphilic drugs as well as genes.[11,12] In particular, amphiphilic diblock copolypeptide (ADC) or protein hybrid copolymers recently received much attention for the fabrication of stimuli-responsive micelles and vesicles for various biomedical applications, such as drug delivery and gene therapy.[13–15]

To effectively deliver the PS, the carrier must also be able to incorporate the PS without loss or alteration of its activity.

Correspondence to: X.-Z. Zhang (E-mail: xz-zhang@whu.edu.cn)

Given the high probability of repetitive dosing schedules, the system must also be biodegradable and have little or no immunogenicity.[16] Amphiphilic micelles based on polypeptide-PS conjugates could satisfied these requirements. Herein, we report a series of porphyrin-functionalized ADCs for PDT, which have high fluorescence quantum yields. The polypeptides synthesized by ROP of NCAs have good biocompatibility and conspicuous PDT efficacy.

EXPERIMENTAL

Materials

N,*N*-Dimethylformamide (DMF; Shanghai Chemical Reagent) was used after distillation under reduced pressure. Tetrahydrofuran (THF; Shanghai Chemical Reagent) was treated with Na and then purified by vacuum distillation before use. *N*(ε)-Benzyloxycarbonyl-L-lysine (H-Lys(Z)-OH; 99%; Aldrich), L-leucine (99%; Aldrich), *n*-hexane (Shanghai Chemical Reagent), trifluoroacetic acid (TFA; 99%; Aldrich), hydrogen bromide (33 wt % in glacial acetic acid; Sigma), and diethyl ether (Shanghai Chemical Reagent) were used as received.

Measurements

The ^{1}H NMR spectra of products were recorded on a Mercury VX-300 spectrometer at 300 MHz (Varian) by using TFA-d and dimethyl sulfoxide-d_6 (DMSO-d_6) as a solvent and tetramethylsilane (TMS) as an internal standard.

Fourier Transform Infrared (FT-IR) spectra were recorded on an AVATAR 360 spectrometer. Samples were pressed into potassium bromide (KBr) pellets.

Synthesis of 5-(4-Aminophenyl)-10,15,20-triphenylporphyrin

5-(4-Aminophenyl)-10,15,20-triphenyl-porphyrin (APP) was synthesized according to the literature procedure.[17–19]

Synthesis of Leu-NCA and Z-Lys-NCA

L-Leucine-*N*-carboxyanhydride (Leu-NCA) and *N*(ε)-Benzyloxycarbonyl-L-lysine-*N*-carboxyanhydride (Z-Lys-NCA) were synthesized according to a literature procedure.[20] L-Leucine (2.62 g, 0.02 mol) was suspended in freshly distilled THF (90 mL) in a 250-mL three-necked flask. The system was magnetically stirred under a steady flow of N_2, then triphosgene (5.94 g, 0.02 mol) in a THF solution (15 mL) was added dropwise to the suspension. Subsequently, the reaction mixture was heated to 50 °C and stirred for 90 min to yield a clear solution. The solution was condensed under reduced pressure and then was poured into excess dried *n*-hexane to obtain crude crystals of Leu-NCA, which were further recrystallized from dried THF/*n*-hexane twice and dried under vacuum. Z-Lys-NCA was synthesized according to a similar procedure.

Synthesis of APP-L_n

APP-poly(L-leucine) (APP-L_n) was prepared by ROP of Leu-NCA initiated by APP in DMF with a feed ratio of 1/80 (APP/Leu-NCA molar ratio). The resultant solution of Leu-NCA and APP was stirred under a N_2 atmosphere for 4 days at 50 °C. The product was purified by dialysis against DMF for 3 days and distilled water for 4 days, and finally freeze-dried.

Synthesis of Poly(L-leucine)-*block*-polylysine (APP-L_nK_m)

The diblock copolymers were prepared by ROP of Z-Lys NCA initiated by the macroinitiator APP-L_n in DMF with feed ratios of 1/1 and 1/2 (Leu-NCA/Z-Lys-NCA molar ratio), respectively. The reaction mixture was stirred under a N_2 atmosphere for 4 days at 50 °C. The products were purified by dialysis against DMF for 3 days and distilled water for 4 days. After freeze-drying, APP-Leucine$_{109}$-*b*-Lysine(Z)$_{107}$ (APP-$L_{109}K(Z)_{107}$) and APP-Leucine$_{109}$-*b*-Lysine(Z)$_{186}$ (APP-$L_{109}K(Z)_{186}$) were obtained from the feed ratios of 1/1 and 1/2 (Leu-NCA/Z-Lys-NCA molar ratio), respectively.

Subsequently, a 100-mL round-bottom flask was charged with APP-$L_{109}K(Z)_{107}$ (155 mg) and TFA (8 mL) and was placed in an ice bath. The mixture was stirred for 15 min. HBr (3 mL of a 33 wt % solution in acetic acid) was then added dropwise and the system was allowed to stir for 1 h. Then diethyl ether (20 mL) was added to precipitate the product. The mixture was centrifuged to isolate the green solid precipitate. After drying, product was resuspended in 10 mL DMF, and the solution was placed in a dialysis bag (Molecular Weight Cut Off (MWCO) = 3500 g mol^{-1}) and dialyzed against distilled water for 4 days (water changed every 8 h). After dialysis, the sample was lyophilized to give the product (APP-$L_{109}K_{107}$) (60.7 mg). Similarly, 57.0 mg of APP-$L_{109}K_{186}$ was obtained after the deprotection of 140 mg APP-$L_{109}K(Z)_{186}$.

Determination of Critical Micelle Concentration

Fluorescence spectra were recorded on a LS55 luminescence spectrometer (PerkinElmer). Pyrene was used as a hydrophobic fluorescent probe.[21] Aliquots of pyrene solutions (1.2×10^{-7} mol mL^{-1} in acetone, 50 μL) were added to containers, and the acetone was allowed to evaporate. One milliliter aqueous solution of polymer with a particular concentration was added to the container, which contained the pyrene residue. The aqueous sample solutions containing pyrene residue at the same concentration of 6×10^{-6} M were kept at room temperature for 24 h to reach the solubilization equilibrium of pyrene in the aqueous phase. Emission wavelength was carried out at 393 nm, and excitation spectra were recorded ranging from 300 to 360 nm. Both excitation and emission slit widths were 10 nm. From the pyrene excitation spectra, the intensity ratio I_{338}/I_{335} was analyzed as a function of logarithm of the polymer concentration. A critical micelle concentration (CMC) value was determined from the intersection of the tangent to the curve at the inflection with the horizontal tangent through the points at low concentration.[22]

Micelle Formation

The micelles of APP-$L_{109}K_{186}$ were prepared by a dialysis method. Briefly, the polymer was dissolved in DMSO at an initial concentration of 200 mg L^{-1} and then dialyzed against distilled water for 2 days using a dialysis bag (MWCO = 3500 g mol^{-1}).

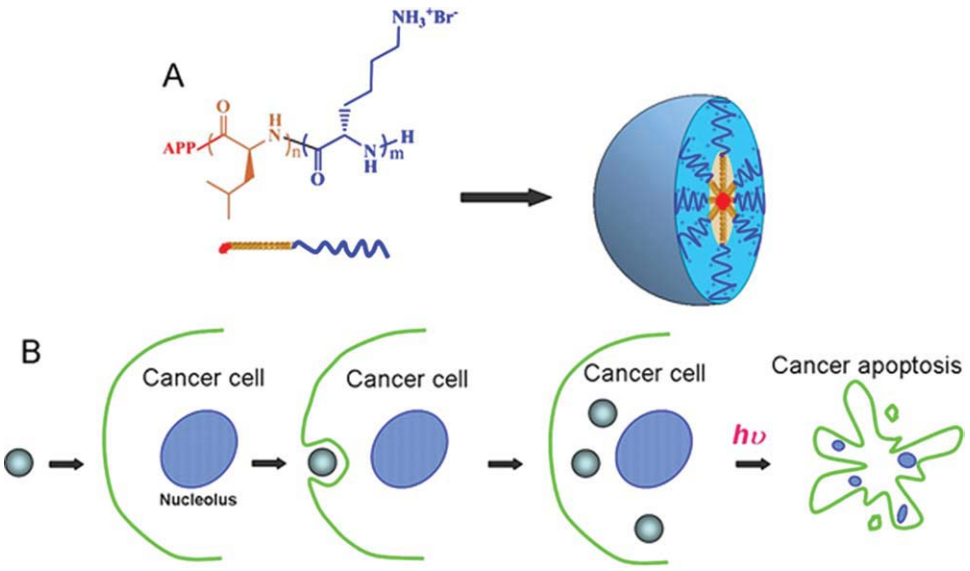

SCHEME 1 Core-shell micelle self-assembled from APP-$L_{109}K_{186}$ with phototoxicity toward cancer cells.

Transmission Electron Microscopy

Transmission electron microscopy (TEM) experiments were carried out on a JEM-100CX II instrument operating at an acceleration voltage of 80 KV. A drop of micelle suspension was placed on a copper grid with formvar film and stained by a 0.2% (w/v) solution of phosphotungstic acid before measurement.

Size Distribution Measurements

Zeta sizer Nano ZS (Malvern Instruments) was used to determine the size and size distribution of self-assembled micelles. The micelle-contained solution (~100 mg L^{-1}) was passed through a 0.45-μm pore size filter before measurement.

Fluorescence Quantum Yields

Fluorescence emission spectra were recorded on a LS55 luminescence spectrometer (PerkinElmer) spectrofluorimeter. The excitation and emission slit widths were both 10 nm. All absorption spectra were acquired using a Lambda Bio40 UV-vis spectrometer (PerkinElmer). All the measurements were performed within 3 h after preparation of the solutions. Stock solutions of tetraphenylporphyrin (H_2TPP, 0.0001 mg mL^{-1} in DMSO), APP-$L_{109}K_{107}$ (0.023 mg mL^{-1} in phosphate buffered saline (PBS) pH 7.4), and APP-$L_{109}K_{186}$ (0.047 mg mL^{-1} in PBS pH 7.4) were prepared. Each solution contains the same concentration of porphyrin. The quantum yields were calculated using a secondary standard method.[23] H_2TPP was used as a secondary standard. According to this approach, the integrated fluorescence intensity of the analyte (I) and standard (I_s), the absorbencies of the analyte (A) and the standard (A_s) at excitation wavelength, the excitation wavelengths of analyte (λ) and the standard (λ_s), and the refractive indexes of analyte solution (n) and standard solution (n_s) are related to the quantum yield of the analyte (ϕ) as follows:

$$\phi = \phi_s \frac{I}{I_s}\frac{A_s}{A}\frac{\lambda_s}{\lambda}\frac{n^2}{n_s^2}$$

where, ϕ_s is the quantum yield of the reference standard (0.11 for H_2TPP).[24]

Dark Cytotoxicity of APP-L_nK_m

In vitro cytotoxicity was evaluated using human hepatocellular liver carcinoma (HepG2) and human cervical carcinoma (HeLa) cells. For dark cytotoxicity assay, 200 μL of cells in Dulbecco's modified eagle medium (DMEM) with a concentration of 2.0×10^4 cells/mL was added to each well (4.0×10^3 cells/well) in a 96-well plate. After incubation for 24 h in incubator (37 °C, 5% CO_2), the culture medium in each well was replaced by 200 μL of DMEM or 4-(2-hydroxyethyl)-1-piperazineethanesulfonic acid (HEPES) buffer, containing the polymer with a particular concentration, and the cells were further incubated for 48 h. Then, the medium was replaced by fresh DMEM or HEPES and 20 μL of 3-(4,5-dimethylthiazol-2-yl)-2,5-diphenyltetrazolium bromide (MTT) solution (5 mg mL^{-1}). After incubation for 4 h, 200 μL of DMSO was added and shaken at room temperature. The optical density (OD) was measured at 570 nm with a Microplate Reader Model550 (BIO-RAD). The viable rate was calculated by the following equation: cell viability = $OD_{treated}/OD_{control}$, where $OD_{control}$ was obtained in the absence of polymer and $OD_{treated}$ was obtained in the presence of polymer.

Phototoxicity of APP-L_nK_m

For phototoxicity assay, the HepG2 cells and HeLa cells were cultured as described above for the dark cytotoxicity assay. After the polymer-contained culture medium was added, the plate with cells was then placed on ice and exposed to light from a 150-W xenon lamp filtered through a 400–700-nm long-pass filter for 20 min. The cells were returned to the incubator overnight and assayed for viability. Other conditions were the same as that for dark cytotoxicity assay.

RESULTS AND DISCUSSION

Synthesis and Characterizations of APP-L_nK_m

In this study, core-shell micelles self-assembled from polymer APP-$L_{109}K_{186}$ with phototoxicity toward cancer cells were prepared (Scheme 1). The polymer synthetic procedures consist of four steps (Scheme 2): the synthesis of

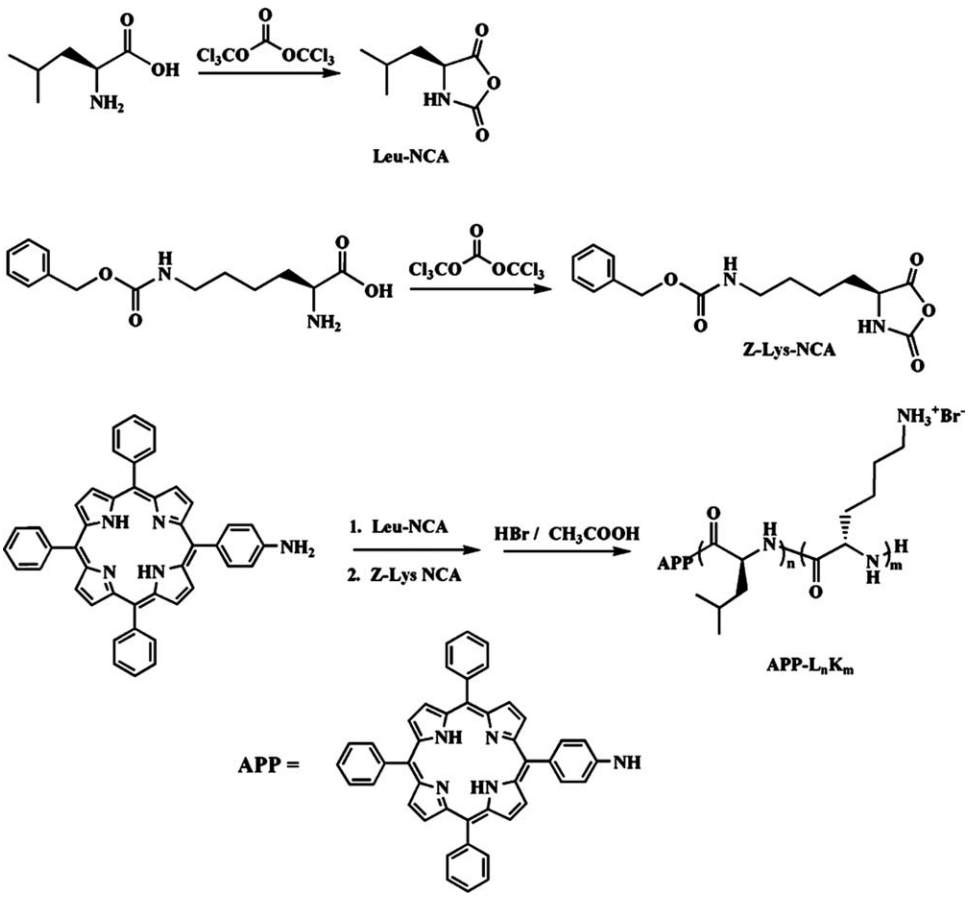

SCHEME 2 Synthesis of Leu-NCA, Z-Lys-NCA, and APP-L_nK_m.

Leu-NCA and Z-Lys-NCA, the synthesis of APP-L_n, the synthesis of APP-$L_nK(Z)_m$, and the deprotection of benzyloxycarbonyl (Z) from APP-$L_nK(Z)_m$. The first step was to prepare two monomers. Their chemical structures were confirmed by ^{1}H NMR (in Fig. 1). The second step was to prepare amino-terminated APP-L_n, which was synthesized by ROP method with APP as an initiator. The chemical structure of APP-L_n was characterized by ^{1}H NMR (in TFA-d) shown in Figure 2. The characteristic signals at 0.94 (a), 1.63 (b), 1.73 (c), and 4.71 ppm (d) are assigned to the protons of leucine units. The characteristic signals at 7–9 ppm (e) are assigned to the porphyrin protons. The integration ratio of the two types of signals indicates that the degree of polymerization is 109 (n = 109, M_n = 13000). The third step was to polymerize the

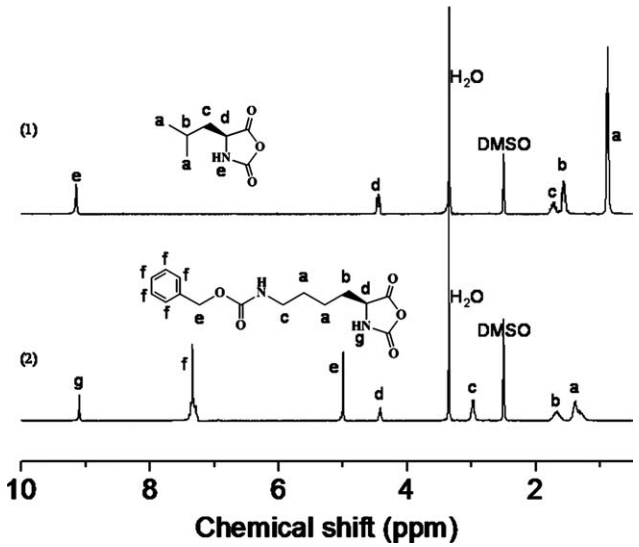

FIGURE 1 ^{1}H NMR spectra of (1) Leu-NCA and (2) Z-Lys-NCA.

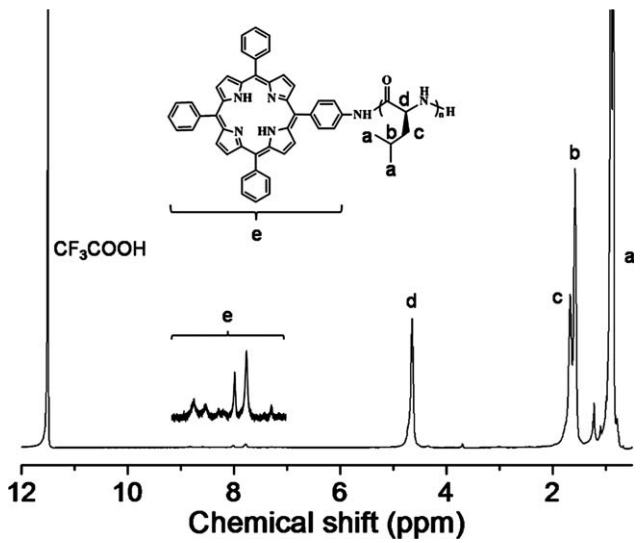

FIGURE 2 ^{1}H NMR spectrum of APP-L_n.

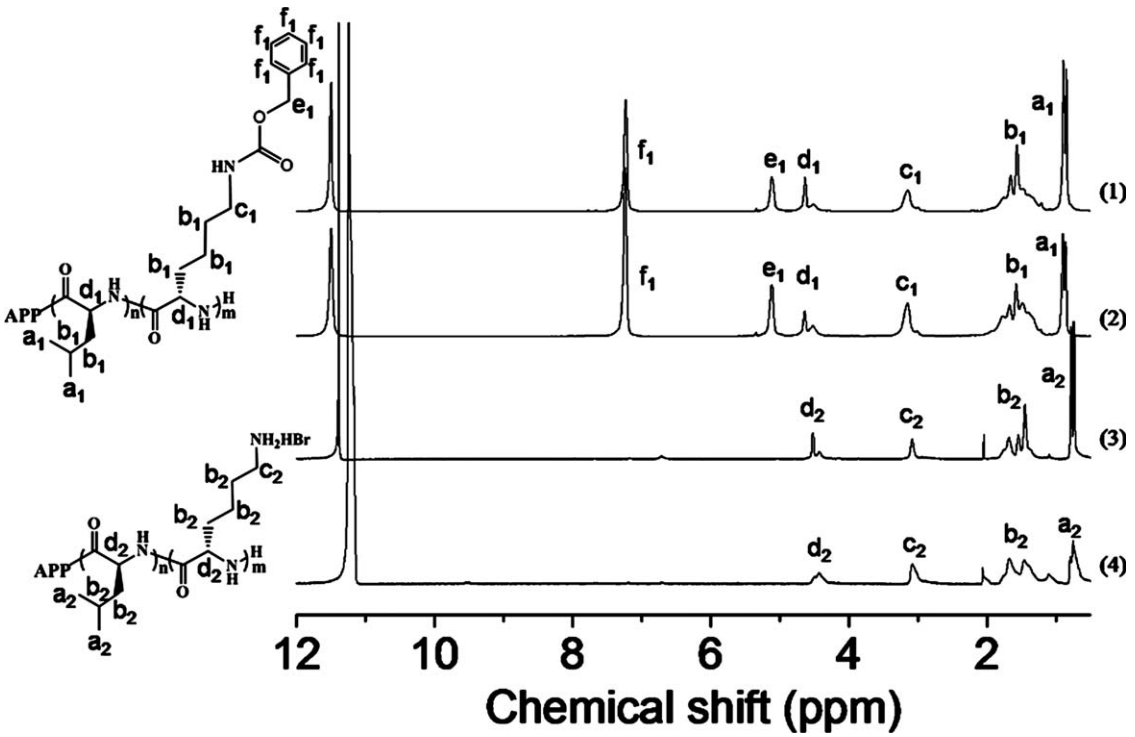

FIGURE 3 ^{1}H NMR spectra of (1) APP-$L_{109}K(Z)_{107}$, (2) APP-$L_{109}K(Z)_{186}$, (3) APP-$L_{109}K_{107}$, and (4) APP-$L_{109}K_{186}$.

second monomer (Z-Lys-NCA) with APP-L_n as a macroinitiator. The structure of APP-$L_nK(Z)_m$ was characterized by ^{1}H NMR (in TFA-d). As shown in Figure 3(1) and (2), the appearance of Z group signals (5.10 and 7.20 ppm) implies that the two types of diblock copolypeptides with different polylysine chain lengths are successfully synthesized. The composition of the diblock copolypeptides are listed in Table 1. Finally, two types of ADCs were obtained after the deprotection of Z groups from APP-$L_nK(Z)_m$. As shown in Figure 3(3) and (4), the disappearance of Z group signals reveals that the two types of polypeptides are successfully obtained. The same conclusion is drawn from the FT-IR spectra. As shown in Figure 4, the peaks at 1650 and 1550 cm^{-1} are attributed to the amide I band and amide II band in the polypeptide chain, respectively.

Micelle Formation and Characterizations

The ADC APP-$L_{109}K_{186}$ could self-assemble into micelles in an aqueous medium. The formation of APP-$L_{109}K_{186}$ micelles was verified by the fluorescence technique using pyrene as a probe. Concomitant with the increase in fluorescence intensity, a red-shift from 335 to 338 nm takes place ascribed to the micellization of the ADCs, because pyrene is preferentially partitioned into the hydrophobic core of the micelles with a change of the photophysical properties. From the plot of fluorescence intensity ratio I_{338}/I_{335} versus the logarithm of polymer concentration in Figure 5, the CMC value is determined to be 30.6 mg L^{-1}.

This micellar structure was further confirmed by TEM. As shown in Figure 6, it is evident that the self-assembled

TABLE 1 Feed Composition and Composition of APP-L_nK_m

Diblock Copolypeptide	APP/Leu-NCA/Z-Lys-NCA Feed Molar Ratio	APP/Leu[a]/Lys[b] Molar Ratio[c] in Diblock Copolypeptide
APP-$L_{109}K_{107}$	1/80/109	1/109/107
APP-$L_{109}K_{186}$	1/80/218	1/109/186

[a] Leucine unit.
[b] Lysine unit.
[c] Calculated from ^{1}H NMR spectra.

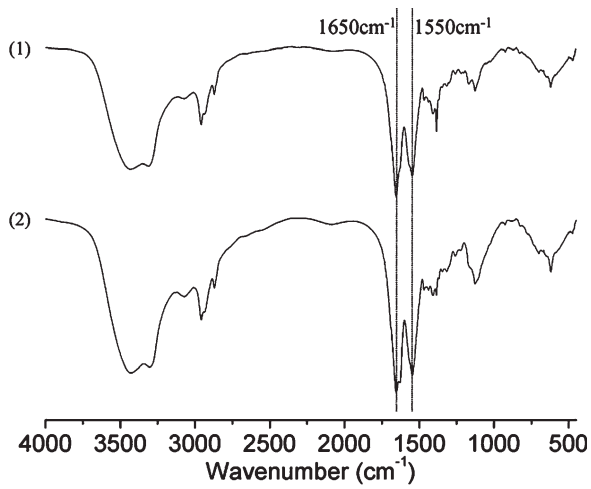

FIGURE 4 FT-IR spectra of (1) APP-$L_{109}K_{107}$ and (2) APP-$L_{109}K_{186}$.

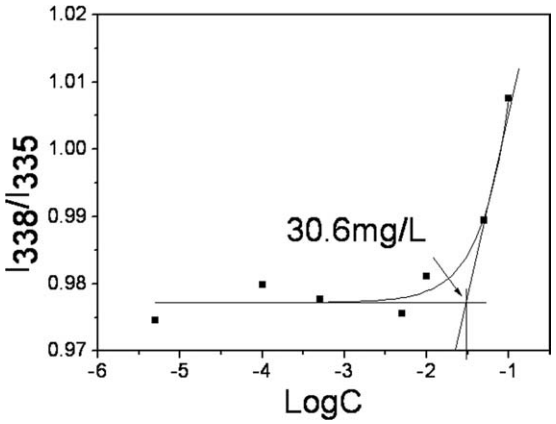

FIGURE 5 The intensity ratio I_{338}/I_{335} in the excitation spectrum as a function of logarithm of APP-$L_{109}K_{186}$ concentration. The CMC is 30.6 mg L^{-1}.

micelles formed have a regular spherical shape and are well-dispersed. From the TEM image, the sizes of micelles are <30 nm. Because of the shorter hydrophilic segments of

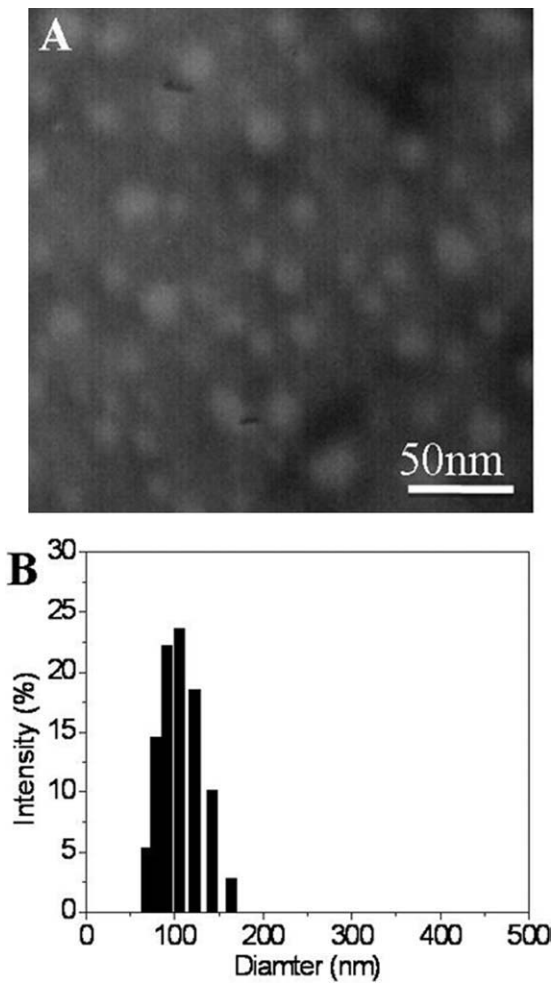

FIGURE 6 TEM image of APP-$L_{109}K_{186}$ (A) micelles self-assembled in aqueous medium and the sizes of micelles determined by DLS (B).

TABLE 2 Fluorescence Quantum Yields of APP-$L_{109}K_{107}$ and APP-$L_{109}K_{186}$ in PBS (pH = 7.4, Excitation at 420 nm, and Emission at 650 nm)

Diblock Copolypeptide	ϕ
APP-$L_{109}K_{107}$	0.24
APP-$L_{109}K_{186}$	0.25

polylysine, the aggregation pattern of APP-$L_{109}K_{107}$ becomes elusive (data not shown). Therefore, we focused our study on the APP-$L_{109}K_{186}$ micelles. From the dynamic light scattering (DLS) shown in Figure 6, the mean size of APP-$L_{109}K_{186}$ micelles is 120 nm. The difference in the sizes determined by different methods is mainly attributed to the fact that the size measured by the DLS is the hydrodynamic diameter of micelles in aqueous solution, while the size observed by TEM is the diameter of the freeze-dried micelles. Similar conclusion was drawn in literature.[25,26]

Fluorescence Quantum Yields

We know that conventional PSs tend to aggregate in aqueous media as a result of their π–π interactions and lipophilic

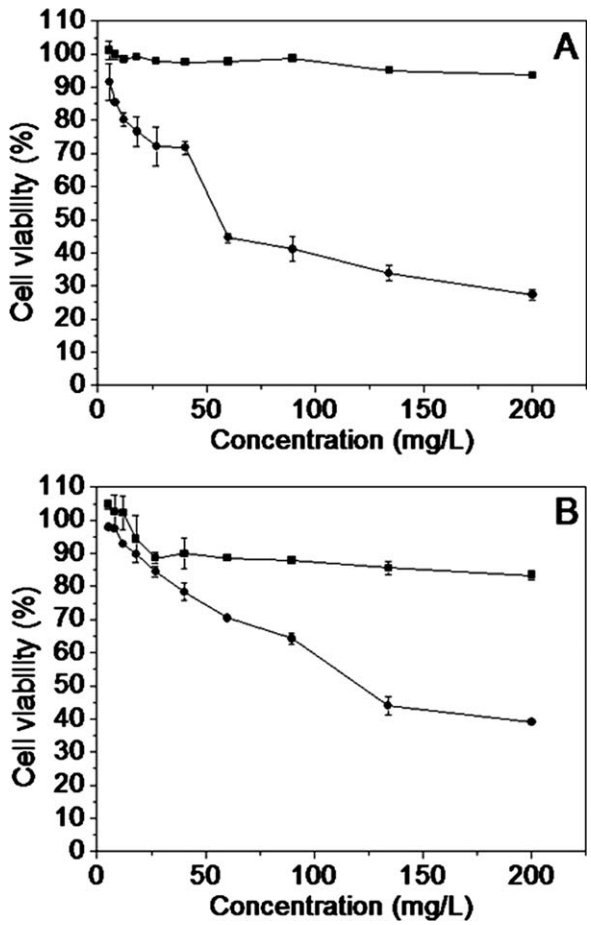

FIGURE 7 Dark toxicity (square labelled line) and phototoxicity (circle labelled line) of polymers for (A) HepG2 cells and (B) HeLa cells.

nature, which affects their efficacy *in vivo* because of the decreased bioavailability and capacity to absorb light, that is, low tendency to aggregation in aqueous media is an important requirement for the photodynamic agents. Herein, we investigated the fluorescence quantum yields of APP-$L_{109}K_{107}$ and APP-$L_{109}K_{186}$. As shown in Table 2, the porphyrin-functionalized diblock copolypeptides show high fluorescence quantum yields. In other words, there is no activity loss or alteration occurred after the porphyrins being incorporated to the diblock copolypeptides.

In Vitro Cytotoxicity

As shown in Figure 7, no significant decrease in cell viability occurs when the concentration of the APP-$L_{109}K_{186}$ is below 200 mg L^{-1} for HepG2 [Fig. 7(A)] and HeLa [Fig. 7(B)] cells. Obviously, APP-$L_{109}K_{186}$ does not show apparent dark cytotoxicity. This is attributed to the self-assembly of the polycationic segments, which greatly diminishes its cytotoxicity.[15] The phenomenon most likely is resulted from chain assembly preventing free diffusion of the polycations to cell surfaces.[27]

In contrast, the ADC exhibits visible phototoxicity toward HepG2 cells and HeLa cells. APP-$L_{109}K_{186}$ shows slightly higher phototoxicity in HepG2 cells than in HeLa cells, The IC_{50} values of APP-$L_{109}K_{186}$ are 60 and 100 mg L^{-1} for HepG2 cells and HeLa cells, respectively.

CONCLUSIONS

In summary, a series of porphyrin-functionalized ADCs were synthesized by ROP of Leu-NCA and Z-Lys-NCA, followed by the deprotection of Z groups. DLS measurements and TEM observation confirmed the micellar structure formed by the self-assembly of the polymer synthesized. APP-$L_{109}K_{186}$ micelles exhibited no significant dark cytotoxicity and high PDT efficacy against HepG2 and HeLa cells. These results indicated APP-$L_{109}K_{186}$ micelles could be a novel carrier for cancer therapy.

This work was supported by the Ministry of Science and Technology of China (2009CB930300), Trans (New)-Century Training Programme Foundation for the Talents from the Ministry of Education of China, and Natural Science Foundation of Hubei Province, China (2009CDA024).

REFERENCES AND NOTES

1 Levy, J. G.; Obochi, M. Photochem Photobiol 1996, 64, 737–739.

2 Dougherty, T. J. Photochem Photobiol 1987, 45, 879–889.

3 Kreimer-Birnbaum, M. Semin Hematol 1989, 26, 157–173.

4 Konan, Y. N.; Gurny, R.; Allemann, E. J Photoch Photobio B 2002, 66, 89–106.

5 Oenbrink, G.; Jurgenlimke, P.; Gabel, D. Photochem Photobiol 1988, 48, 451–456.

6 Rosenthal, I. Photochem Photobiol 1991, 53, 859–870.

7 Brasseur, N.; Ali, H.; Langlois, R.; Van Lier, J. E. Photochem Photobiol 1988, 47, 705–711.

8 Isele, U.; Schieweck, K.; Van Hoogevest, P.; Capraro, H. G.; Kessler, R. J Pharm Sci 1995, 84, 166–173.

9 Leuchs, H. Ber Dtsch Chem Ges 1906, 39, 857–861.

10 Kricheldorf, H. R. Angew Chem Int Edit 2006, 45, 5752–5784.

11 Allen, C.; Maysinger, D.; Eisenberg, A. Colloid Surface B 1999, 16, 3–27.

12 Gref, R.; Minamitake, Y.; Peracchia, M. T.; Trubetskoy, V.; Torchilin, V.; Langer, R. Science 1994, 263, 1600–1603.

13 Bae, Y.; Kataoka, K. Adv Drug Deliver Rev 2009, 61, 768–784.

14 Osada, K.; Kataoka, K. Adv Polym Sci 2006, 202, 113–153.

15 Holowka, E. P.; Sun, V. Z.; Kamei, D. T.; Deming, T. J. Nat Mater 2007, 6, 52–57.

16 Poste, G.; Kirsh, R. Nat Biotechnol 1983, 1, 869–878.

17 Adler, A. D.; Longo, F. R.; Shergalis, W. J Am Chem Soc 1964, 86, 3145–3149.

18 Kruper, W. J.; Chamberlin, T. A.; Kochanny, M. J Org Chem 1989, 54, 2753–2756.

19 Wu, D. Q.; Li, Z. Y.; Li, C.; Fan, J. J.; Lu, B.; Chang, C.; Cheng, S. X.; Zhang, X. Z.; Zhuo, R. X. Pharm Res 2010, 27, 187–199.

20 Daly, W. H.; Poche, D. Tetrahedron Lett 1988, 29, 5859–5862.

21 Hu, X. L.; Liu, S.; Chen, X. S.; Mo, G. J.; Xie, Z. G.; Jing, X. B. Biomacromolecules 2008, 9, 553–560.

22 Liu, Y. H.; Cao, X. H.; Luo, M. B.; Le, Z. G.; Xu, W. Y. J Colloid Interface Sci 2009, 329, 244–252.

23 Fery-Forgues, S.; Lavabre, D. J Chem Educ 1999, 76, 1260–1264.

24 Seybold, P. G.; Gouterman, M. J Mol Spectrosc 1969, 31, 1–13.

25 Morita, T.; Horikiri, Y.; Suzuki, T.; Yoshino, H. Int J Pharm 2001, 219, 127–137.

26 Giacomelli, C.; Schmidt, V.; Borsali, R. Macromolecules 2007, 40, 2148–2157.

27 Pakstis, L. M.; Ozbas, B.; Hales, K. D.; Nowak, A. P.; Deming, T. J.; Pochan, D. Biomacromolecules 2004, 5, 312–318.